Resource

Chemistry & Biology

Quantitative Lipoproteomics in *Clostridium difficile* Reveals a Role for Lipoproteins in Sporulation

Graphical Abstract

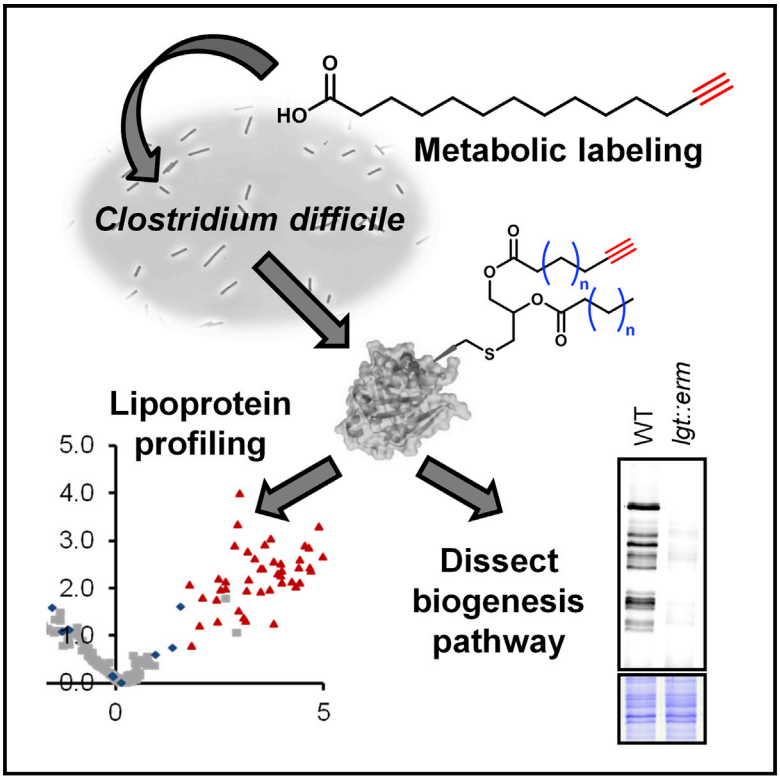

Highlights

- Alkyne-tagged myristate is an efficient probe for *C. difficile* lipoproteins
- Quantitative chemical proteomics enables lipoproteome profiling in diverse strains
- Chemical and genetic inactivation demonstrated the activity of an accessory LspA
- A vital role for the lipoproteome in sporulation has been identified

Authors

Thomas M. Charlton, Andrea Kovacs-Simon, Stephen L. Michell, Neil F. Fairweather, Edward W. Tate

Correspondence

e.tate@imperial.ac.uk (E.W.T.), n.fairweather@imperial.ac.uk (N.F.F.)

In Brief

Bacterial lipoproteins are *S*-diacylglyceryl modified, surface anchored proteins, which play important roles at the host-pathogen interface. We use metabolic tagging, combined with inactivation of lipoprotein biosynthesis, to profile the *Clostridium difficile* lipoproteome, revealing a role for lipoproteins in transmission of this pathogen.

Accession Numbers

PXD002426

Charlton et al., 2015, Chemistry & Biology *22*, 1562–1573
November 19, 2015 ©2015 The Authors
http://dx.doi.org/10.1016/j.chembiol.2015.10.006

CellPress

Chemistry & Biology
Resource

Quantitative Lipoproteomics in *Clostridium difficile* Reveals a Role for Lipoproteins in Sporulation

Thomas M. Charlton,[1,2,3] Andrea Kovacs-Simon,[4] Stephen L. Michell,[4] Neil F. Fairweather,[2,3,*] and Edward W. Tate[1,3,*]
[1]Department of Chemistry, Imperial College London, London SW7 2AZ, UK
[2]Life Sciences, Imperial College London, London SW7 2AZ, UK
[3]Institute of Chemical Biology, Imperial College London, London SW7 2AZ, UK
[4]Department of Biosciences, College of Life and Environmental Sciences, University of Exeter, Exeter EX4 4QD, UK
*Correspondence: e.tate@imperial.ac.uk (E.W.T.), n.fairweather@imperial.ac.uk (N.F.F.)
http://dx.doi.org/10.1016/j.chembiol.2015.10.006

SUMMARY

Bacterial lipoproteins are surface exposed, anchored to the membrane by *S*-diacylglyceryl modification of the N-terminal cysteine thiol. They play important roles in many essential cellular processes and in bacterial pathogenesis. For example, *Clostridium difficile* is a Gram-positive anaerobe that causes severe gastrointestinal disease; however, its lipoproteome remains poorly characterized. Here we describe the application of metabolic tagging with alkyne-tagged lipid analogs, in combination with quantitative proteomics, to profile protein lipidation across diverse *C. difficile* strains and on inactivation of specific components of the lipoprotein biogenesis pathway. These studies provide the first comprehensive map of the *C. difficile* lipoproteome, demonstrate the existence of two active lipoprotein signal peptidases, and provide insights into lipoprotein function, implicating the lipoproteome in transmission of this pathogen.

INTRODUCTION

Bacterial lipoproteins are surface-exposed proteins, anchored to the cell membrane through a post-translational diacylglyceryl modification, and participate in diverse cellular processes, including nutrient uptake and transport, cell wall remodeling, sporulation, signaling, adhesion, and antibiotic resistance (Chimalapati et al., 2012; Nielsen and Lampen, 1982; Okugawa et al., 2012). In addition, they can activate host immune response pathways via recognition of the diacylglyceryl motif by Toll-Like Receptor 2 (Blanc et al., 2013).

Gram-positive lipoproteins contain an N-terminal lipobox within their type II signal peptide sequence, which features an invariant +1 cysteine residue (Buddelmeijer, 2015; Hutchings et al., 2009). Following export via the general secretory pathway (Sec), the signal peptide is retained within the membrane and a prolipoprotein diacylglyceryl transferase (Lgt) catalyzes the covalent attachment of a membrane phospholipid substrate to the conserved cysteine, forming a thioether linkage (Sankaran and Wu, 1994). The signal peptide is cleaved by a lipoprotein (type II) signal peptidase (Lsp) (Hayashi et al., 1985), leaving the mature lipoprotein anchored to the membrane via the lipid-modified N-terminal cysteine (Figure 1). Lgt and Lsp are essential in Gram-negative bacteria, but are dispensable in Gram-positive bacteria studied to date, despite the essential nature of many lipoproteins (Widdick et al., 2011).

Previous methods for studying bacterial lipoproteins rely on radiolabeling with fatty acids, which suffers from low sensitivity and relatively low throughput. Consequently, bioinformatics prediction is commonly used but is restricted to proteins containing a well-defined lipobox motif and requires experimental confirmation (Rahman et al., 2008). Disruption of lipoprotein processing by genetic inactivation of *lgt* (Baumgartner et al., 2007) or by inhibition of Lsp by the antibiotic globomycin (Reglier-Poupet et al., 2003) have enabled identification of a small number of lipoproteins, but these approaches lack general applicability. In contrast, metabolic chemical tagging with alkyne-tagged fatty acid analogs provides a potentially global approach to study the lipoproteome, as demonstrated in proof of principle studies in diverse species of Gram-negatives, Gram-positives, and *Mycobacteria* (Rangan et al., 2010).

Metabolic tagging takes advantage of the cell's post-translational machinery to incorporate a chemical tag specifically at the site of modification, allowing visualization and identification of a certain class of post-translational modification (PTM) (Tate et al., 2015). Typically, an analog of the natural substrate featuring a biologically unobtrusive tag (e.g. azide or alkyne) is used. Attachment of a fluorophore through a highly selective, so-called bio-orthogonal, reaction enables rapid and sensitive detection of labeled proteins, while attachment of an affinity tag allows selective and efficient enrichment of labeled proteins for identification by tandem mass spectrometry (MS/MS)-based proteomic analysis. This approach has been applied to the study of a range of PTMs, including acetylation (Yang et al., 2010), myristoylation (Broncel et al., 2015; Charron et al., 2009; Thinon et al., 2014; Wright et al., 2014), palmitoylation (Charron et al., 2009; Martin et al., 2012), cholesterylation (Ciepla et al., 2014), and prenylation (Berry et al., 2010; Charron et al., 2013). However, metabolic tagging and MS/MS-based identification of the lipoproteome has not previously been applied to a Gram-positive bacterium or to pathogenic bacteria.

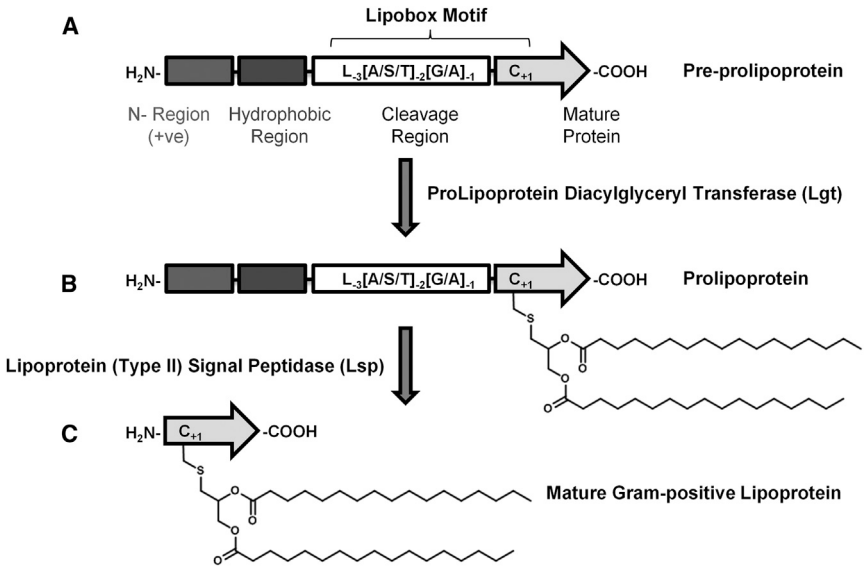

Figure 1. Lipoprotein Biogenesis in Gram-Positive Bacteria

(A) Prolipoprotein diacylglyceryl transferase (Lgt) catalyzes the addition of a diacylglyceryl fatty acid to the invariant lipobox cysteine side chain.

(B) The N-terminal type II signal peptide is cleaved within the lipobox, leaving the conserved cysteine as the N-terminal residue.

(C) The mature lipoprotein remains anchored to the membrane via the lipid modification.

Clostridium difficile is a Gram-positive, spore-forming, anaerobe that causes severe gastrointestinal disease. It is highly antibiotic resistant and is the leading cause of hospital-acquired infection (Kuipers and Surawicz, 2008). *C. difficile* infection (CDI) typically occurs following broad-spectrum antibiotic treatment, which disrupts the natural gut microbiota and enables colonization (Evans and Safdar, 2015). *C. difficile* cells produce two toxins, TcdA and B, which are the major virulence factors (Jank and Aktories, 2008) and lead to symptomatic infection. Spores produced in the gastrointestinal tract of the host during infection are shed in feces (Lawley et al., 2009), and are responsible for persistence and recurrence of CDI due to their resistance to disinfectants, desiccation, and extreme temperatures (Gerding et al., 2008). The *C. difficile* lipoproteome is expected to play an important role in CDI through modulation of host-pathogen interactions, nutrient uptake, and sporulation. For example, the predicted lipoprotein CD630_08730 is a surface-exposed adhesin anticipated to have an important role during colonization (Kovacs-Simon et al., 2014), while expression of the putative lipoproteins OppA and AppA indirectly inhibits sporulation, suggesting that these proteins may modulate virulence by controlling nutrient availability (Edwards et al., 2014).

Here we report the first global study of the *C. difficile* lipoproteome using metabolic tagging and quantitative proteomic profiling. We demonstrate experimentally the lipidation of over 50 lipoproteins in two strains and analyze the effects of mutation of three genes essential for lipoprotein lipidation and proteolytic processing. Furthermore, we describe a sporulation defect in these mutants and identify lipoproteins implicated in sporulation, highlighting the power of this approach for lipoprotein identification and characterization in this important human pathogen.

RESULTS

Alkyne-Tagged Myristate Is an Efficient Probe for *C. difficile* Lipoproteins

We used metabolic tagging with an alkyne-tagged fatty acid analog, in conjunction with quantitative proteomics, to create a comprehensive profile of the lipoproteome of *C. difficile* 630 Δ*erm*. Lgt enzymes typically exhibit little selectivity with respect to the lipid substrate, accepting saturated or mono-unsaturated fatty acids of 14–20 carbons (Nakayama et al., 2012). We therefore used a series of alkyne-tagged fatty acid analogs of increasing chain length (C_{11}, C_{12}, C_{13}, C_{14}, C_{17}, and C_{18}), synthesized following a route previously reported by our group (Wright et al., 2014). Exponential cultures of *C. difficile* 630 were treated with each probe at 25 μM, and incorporation into lipoproteins was assessed by in-gel fluorescence following selective ligation to a multifunctional capture reagent (AzTB) through copper (I)-catalyzed azide-alkyne cycloaddition (CuAAC) as previously described (Broncel et al., 2015). Ligation to AzTB permits both fluorescent detection, through a TAMRA label, and affinity enrichment of tagged proteins, through a PEG-Biotin label. A clear preference for longer chain lengths was observed (Figure S1A) and alkyne-tagged myristic acid (YnMyr) (Figure 2A) was selected for investigation of optimal feeding concentration. A dose of 10 or 25 μM YnMyr gave the strongest labeling, while a reduction in labeling was seen at concentrations higher than 50 μM, possibly due to limitations of probe solubility (Figure S1B). Pronase treatment and western blotting using an anti-lipoteichoic acid (LTA) antibody (Cox et al., 2013) showed that these probes are also incorporated into LTA, an α-D-GlcNAc(1–3)-α-D-GlcNAc glycosyl-phosphate polymer anchored to the cell membrane by a diacylglyceryl anchor (Reid et al., 2012). Methanol/chloroform precipitation prior to CuAAC effectively removed LTA from the sample, enabling affinity enrichment of labeled proteins on NeutrAvidin resin (Figures S1C and S1D).

As lipoproteins potentially play an important role in infection, we compared the labeled lipoproteome of strain 630 with a range of clinical isolates of different ribotypes. A broadly similar labeling pattern was observed for most strains with the exception of the evolutionarily divergent strain M120 and the ribotype 027 strain R20291 (Stabler et al., 2009), which displayed a subtly different profile to 630 (Figure 2B).

Profiling the Lipoproteome of *C. difficile* 630 Δ*erm*

To support lipoproteome profiling, lists of 68 and 62 potential lipoproteins from *C. difficile* strains 630 and R20291, respectively, were generated using bioinformatics methods (Table S1). Broadly conserved putative functions indicated a degree of lipoproteome conservation across these strains,

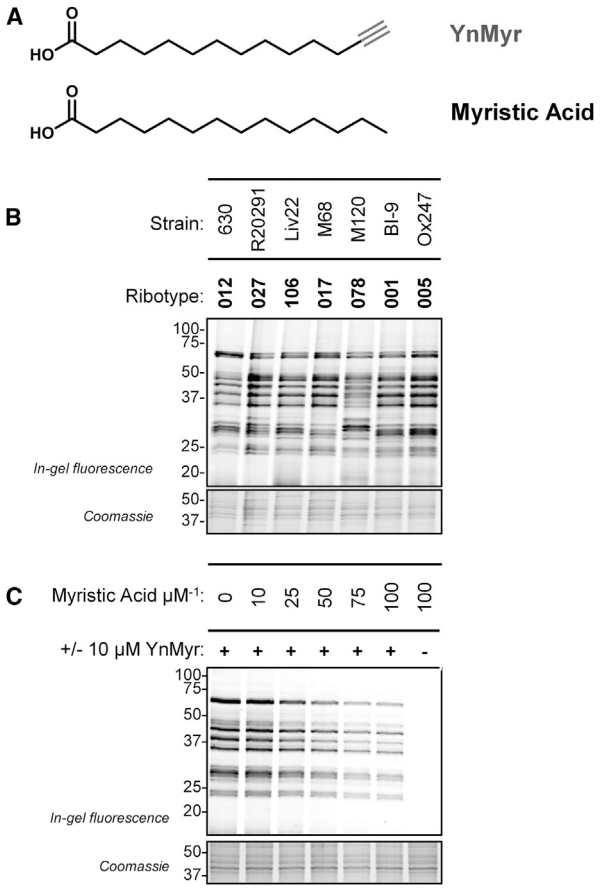

Figure 2. Development and Optimization of Metabolic Tagging to Target Lipidation in *C. difficile*

(A) The structure of the alkyne-tagged myristic acid analog, YnMyr, in comparison to the natural lipid.

(B) Qualitative comparison between the lipoproteomes of *C. difficile* strains of representative ribotypes, visualized by metabolic tagging with 25 μM YnMyr.

(C) Competition between 10 μM YnMyr and up to 100 μM myristic acid, as indicated.

with approximately 1.8% of the proteome predicted to be lipidated.

As genuine protein tagging through modification with YnMyr-containing phospholipids would be expected to be outcompeted by addition of excess myristate, we implemented a quantitative competition analysis in order to focus our lipoprotein profile on valid substrates for lipidation. When *C. difficile* 630 Δ*erm* (a derivative of 630 amenable to genetic manipulation (Heap et al., 2007)) was grown in the presence of 0–100 μM myristic acid and 10 μM YnMyr, a myristate-dependent reduction in in-gel fluorescence was observed (Figure 2C). Based on these results, reduction in biotin-NeutrAvidin enrichment of proteins tagged with 10 μM YnMyr was quantified through triplex dimethyl labeling (Boersema et al., 2009; Li et al., 2013) at 0, 50, and 100 μM competing myristic acid. A total of 187 enriched proteins were quantified in all three biological replicates, and 56 proteins showed a highly significant (multiple ANOVA; $p \leq 0.01$) reduction in enrichment on competition with an excess of myristic acid (Table S2 and Figure 3A). Of these, 46 (82%) were predicted to be lipoproteins by bioinformatics analysis, distributed across a range of known or predicted functions (Table 1 and Figure 3B). Sixty-eight percent of the predicted lipoproteome was identified, representing excellent coverage since not all predicted lipoproteins are expected to be expressed under a single set of experimental conditions. Conversely, it is also possible that a proportion of predicted lipoproteins are not, in fact, genuine substrates for Lgt.

The majority of identified lipoproteins are solute-binding proteins associated with ABC transporters (19), which frequently play an important role in nutrient uptake and are known to be lipidated in other species (Alloing et al., 1994), alongside uncharacterized proteins (4) or putative lipoproteins (14) of unknown function. CD630_08730, an ABC-type transporter sugar-family extracellular solute-binding protein, was significantly outcompeted by excess myristic acid, providing the first direct evidence that this is a lipoprotein. CD630_08730 has been shown to function as an adhesin and a *C. difficile* mutant is unable to adhere to Caco-2 cells, whereas the recombinant protein binds directly to cells (Kovacs-Simon et al., 2014), suggesting that this and other lipoproteins may play important roles in colonization.

We also identified the extracellular chaperones PrsA (CD630_35000) and PrsA2 (CD630_15570) as lipoproteins; PrsA is lipidated in *Bacillus subtilis* and is essential in a number of bacterial species (Kontinen and Sarvas, 1993). These proteins have peptidylprolyl isomerase function and form part of the Sec secretion system, assisting in the folding of exported proteins. Their identification is important as the secondary Sec system in *C. difficile* functions as the major export pathway for the S-Layer Proteins (SLPs), and both Sec systems are essential in *C. difficile* 630 (Fagan and Fairweather, 2011). It is probable that one or both *C. difficile* PrsA proteins play an essential role in the export and folding of the SLPs.

Ten proteins (18%) not predicted to be lipidated by bioinformatics analysis were identified as hits, of which four were predicted to have multiple transmembrane domains and therefore are unlikely to be lipidated by Lgt. We hypothesize that these proteins may show enrichment and myristate-dependent competition due to close association with a lipoprotein or residual-tagged LTA. For example, a calcium-transporting ABC-type transporter ATPase (CD630_16370) was identified in our analysis, and would be expected to be in close association with a solute-binding lipoprotein. Two proteins, CD630_18710 and CD630_19300, have lipoboxes which, in the case of CD630_19300, perfectly match the consensus. CD630_18710 has a predicted signal peptide, but a poorly conserved lipobox, while CD630_19300 has an unusually long signal peptide sequence, neither of which were correctly identified, highlighting the limitations of a purely bioinformatics approach.

Profiling the Lipoproteome of *C. difficile* R20291

The myristate competition experiment was next applied to *C. difficile* R20291, an "epidemic" strain associated with poor clinical outcomes (Stabler et al., 2009) and containing over 230 unique genes compared with strain 630. A total of 110 proteins were quantified in all three biological repeats,

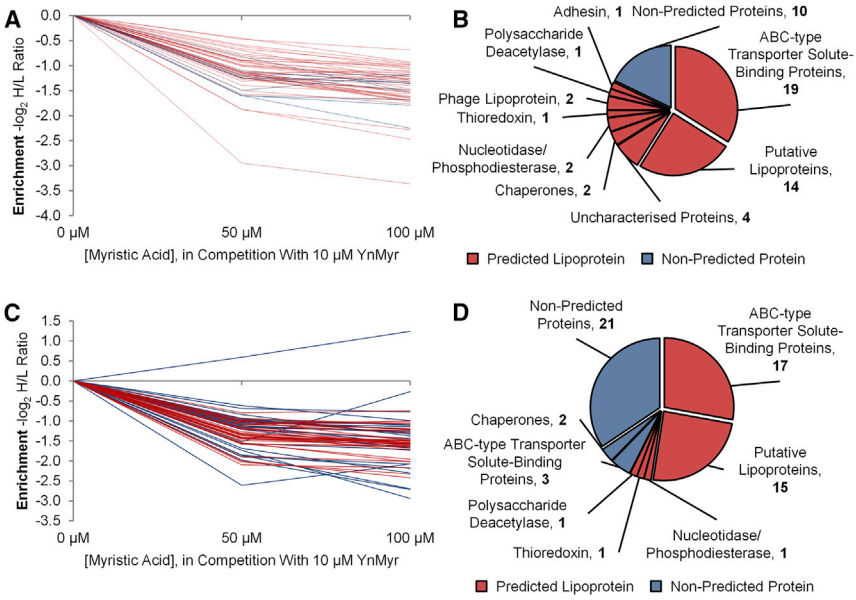

Figure 3. Quantitative Proteomic Analysis of YnMyr-Tagged Proteins in *C. difficile* 630 and R20291

(A) A profile plot showing all proteins from 630 Δ*erm* which showed a significant change in enrichment on competition (multiple ANOVA, $p \leq 0.01$), data represent the mean of three biological replicates; error bars are omitted for clarity.

(B) The annotated functions for the proteins represented in (A); emphasis is placed on predicted lipoproteins.

(C) A profile plot showing all proteins from R20291 that showed a significant change in enrichment on competition (multiple ANOVA, $p \leq 0.01$), data represent the mean of three biological replicates; error bars are omitted for clarity. Pyc (CDR20291_0010), an endogenously biotinylated protein, shows increased enrichment on competition of lipoprotein labeling.

(D) The annotated functions for the proteins represented in (C); emphasis is placed on predicted lipoproteins. Predicted lipoproteins are colored red, other significant proteins in blue.

60 of which showed a significant reduction in enrichment (multiple ANOVA; $p \leq 0.01$) on competition with excess myristic acid (Table S2 and Figure 3C), 35 (57%) of which were predicted to be lipoproteins by bioinformatics analysis, as summarized in Figure 3D. The remaining 25 (43%) were not predicted to be lipidated; 5 of these (8% of total) are homologs of predicted lipoproteins in *C. difficile* 630, including the extracellular chaperones PrsA and PrsA2 and the ABC-type transporter solute-binding proteins SsuA and AppA. In all cases the bioinformatics predictions failed due to incorrect assignment of translation start codons during annotation. The remaining 20 (33%) appear to be background proteins; this level of background enrichment may reflect a need for further optimization of this method for application to R20291. Overall, this result demonstrates that lipoproteins show a high degree of conservation, both functionally and at a primary sequence level, between these two *C. difficile* strains.

Lgt Catalyzes Lipidation in *C. difficile*

C. difficile 630 encodes a single *lgt* gene (CD630_26590). In a 630 Δ*erm lgt::erm* mutant (see Supplemental Information) an almost complete loss of metabolic tagging was observed by in-gel fluorescence, while complementation with a plasmid expressing *lgt* restored the wild-type labeling pattern (Figures 4A and 4C). The *lgt* mutant and wild-type strains had similar growth rates in exponential phase as measured by optical density (data not shown). Comparison of the lipoproteomes of 630 Δ*erm* and *lgt::erm* by quantitative proteomics identified a total of 210 proteins quantified in all three repeats, of which 43 proteins showed significantly increased enrichment in 630 Δ*erm* over *lgt::erm* ($p \leq 0.05$), and 41 were predicted lipoproteins (Tables 1 and S3; Figures 4D and 4E). All but one of the predicted lipoproteins that were significantly enriched in 630 Δ*erm* over *lgt::erm* showed a significant reduction in enrichment on competition with YnMyr and myristic acid, demonstrating unequivocally that these proteins are labeled by YnMyr in an Lgt-dependent manner and are therefore genuine lipoproteins.

The usefulness of the labeling approach is demonstrated by the identification of CD603_18710, a protein not predicted to be lipidated, but significantly enriched through tagging in 630 Δ*erm* compared with *lgt::erm*. We verified lipidation by inducible expression of a C-terminal His_6-tagged protein in both 630 Δ*erm* and *lgt::erm* backgrounds. On induction, CD630_18710-His_6 was highly expressed in both strains, and tagging with YnMyr occurred in an Lgt-dependent manner (Figure S2C). Although we have not identified the site of modification, these multiple lines of evidence strongly suggest that lipidation of CD630_18710 occurs via the canonical pathway despite its non-consensus lipobox.

In other bacterial species, *lgt* mutants can shed lipoproteins into the media at an increased level relative to the wild-type, a phenotype previously used to identify lipoproteins indirectly (Baumgartner et al., 2007; Pribyl et al., 2014). In *C. difficile*, an increase in the amount of protein shed was observed for *lgt::erm*, relative to 630 Δ*erm* (Figure 5A). Western blotting revealed that the SLPs Cwp66 and LMW-SLP were also shed at an increased rate by *lgt::erm* (Figure S5A). We further identified and quantified shed proteins by proteomic analysis, normalized to total protein recovered; 164 proteins were quantified (Figures 5B and S5; Table S4) and, as anticipated, 23 of 24 proteins shed into the media at a significantly ($p \leq 0.05$) increased level by *lgt::erm* relative to 630 Δ*erm* were lipoproteins (Table 1 and Figure 5C). Only 50% of lipoproteins identified through tagging could be detected by this untargeted method, demonstrating a further advantage of enrichment through metabolic chemical tagging over this traditional method for lipoprotein identification.

Two Functional Lipoprotein Signal Peptidases Operate in *C. difficile*

C. difficile 630 encodes two potential *lsp* genes, CD630_25970 (*lspA*) and CD630_19030 (*lspA2*). The existence of two *lspA* genes is highly unusual, but both are conserved across all *C. difficile* strains sequenced to date. Although some other Gram-positive bacteria encode more than one *lsp* gene, the

accessory Lsp may not be functional in all cases (Kovacs-Simon et al., 2011). The existence of two functional LspAs was investigated by insertionally inactivating either *lspA* or *lspA2* in *C. difficile* 630 Δ*erm*; inactivation of either *lspA* or *lspA2* did not affect exponential growth rates (data not shown). The in-gel fluorescence pattern for *lspA::erm* showed a number of lipoprotein bands at higher apparent molecular weight (MW) (Figure 4A), which we hypothesize is due to the retention of the type II signal peptide. Inactivation of *lspA2*, in contrast, resulted in a general reduction in labeling intensity, but relatively few bands shifted to a higher MW. Constitutive expression of *lspA* or *lspA2 in trans* largely restored the wild-type pattern. These data are consistent with LspA processing the majority of lipoproteins, including a number of unique substrates; in contrast, LspA2 may not have unique substrates.

Since double knockouts have, until recently, been very challenging to produce in *C. difficile*, we used a globomycin, a cyclic peptide antibiotic and a specific inhibitor of *Escherichia coli* LspA (Hussain et al., 1980), to further unravel the activity and potential functional redundancy of LspA and LspA2. 630 Δ*erm*, *lspA::erm*, and *lspA2::erm* were grown in the presence 100 μg ml^{-1} globomycin, and the effect on lipoprotein processing was investigated by labeling with 25 μM YnMyr. Treatment with globomycin had no effect on bacterial growth (data not shown). On globomycin treatment, 630 Δ*erm* displayed a remarkably similar labeling pattern to untreated *lspA::erm*, while *lspA::erm*, which possesses only LspA2, showed no significant changes. In contrast, *lspA2::erm* showed dramatic changes when treated with globomycin, with a global shift to higher apparent MWs of YnMyr-tagged lipoproteins (Figure 4B). LspA is thus strongly inhibited by 100 μg ml^{-1} globomycin, while LspA2 is not, a conclusion consistent with the lower sequence homology of *E. coli* K12 LspA to *C. difficile* LspA2, compared with *C. difficile* LspA. Globomycin treatment results in an *lspA::erm*-like phenotype for the parental strain and a doubly inactivated phenotype for *lspA2::erm*, while *lspA::erm* is unaffected by globomycin treatment. Based on these data, we hypothesize that inactivation of both LspAs (*lspA2::erm* + globomycin) results in a global retention of signal peptides and a corresponding migration of labeled lipoproteins at a higher MW that is not observed for individual inactivation of either LspA, strongly suggesting that both LspA and LspA2 have type II signal peptidase activity.

A quantitative lipoproteome analysis between *lspA::erm*, *lspA2::erm*, and 630 Δ*erm* was performed; the majority of the 46 predicted lipoproteins quantified showed no significant change in enrichment between the three strains ($p \leq 0.01$), suggesting that the changes in the in-gel fluorescence band pattern are due to retention of type II signal peptides (Figure S3 and Table S4). An unexpected increase in shedding of proteins into the media was also observed for *lspA::erm* and *lspA2::*erm, relative to 630 Δ*erm* (Figures 5A and S4). A quantitative proteomic comparison between the proteins shed by these mutants revealed that those shed at a significantly ($p \leq 0.05$) increased level by the *lsp* mutants were not lipoproteins (Table S5).

Disrupting Lipoprotein Biogenesis Reduces the Formation of Heat-Resistant Spores

Spo0A (CD630_12140) is a transcription factor that acts as the master control regulator for the initiation of sporulation. When activated by phosphorylation Spo0A∼P binds directly to the DNA upstream of its targets, activating early sporulation genes and repressing those required for stationary phase growth (Edwards and McBride, 2014). Mutants in *spo0A* are defective in sporulation (Underwood et al., 2009) and unable to persist in mice or transmit between animals (Deakin et al., 2012). Incomplete lipoprotein processing in *C. difficile* 630 Δ*erm* resulted in a significant ($p \leq 0.05$) decrease in Spo0A level for *lspA::erm* and *lspA2::erm* of 2.5- and 4.3-fold, respectively, and a 2.2-fold reduction for *lgt::erm*, which approached significance ($p \leq 0.06$), assessed by quantitative proteomic analysis of the global proteomes (Figure 6A; Tables S3 and S4).

The lipoprotein biogenesis mutants produced a similar number of total colony-forming units (CFUs) per milliliter of culture after 16 hr and at all further time points. However, *lgt::erm* and *lspA::erm* exhibited a striking delay in the production of heat-resistant spores, and significantly fewer heat-resistant CFUs ($p \leq 0.05$ at 48 hr; $p \leq 0.01$ thereafter) were formed than by the parental strain, while *lspA2::erm* did not form spores under these conditions (Figure 6B), a result also confirmed by phase-contrast microscopy (Figure S6). The lack of characteristic phase bright spores for *lgt::erm*, *lspA::erm*, and *lspA2::erm* indicates a profound defect in sporulation.

Spo0A Regulation of Lipoprotein Expression in *C. difficile* 630 Δ*erm*

The observed reduction in Spo0A levels in the *lgt::erm*, *lspA::erm*, and *lspA2::erm* mutant strains may in turn affect transcription of Spo0A-regulated genes that encode lipoproteins. In the absence of Spo0A, a number of lipoproteins showed changes in production or lipidation level as assessed by in-gel fluorescence, implying regulation by Spo0A (Figure 6C). To further investigate potential effects on the lipoproteome, and to identify sporulation-associated lipoproteins, a quantitative lipoproteome analysis was performed between *spo0A::erm* and the parental strain, 630 Δ*erm*. Forty-six of the 168 proteins quantified were lipoproteins, and an additional nine previously showed significantly reduced enrichment on competition between YnMyr and excess myristate. Four ABC-type transporter solute-binding proteins were significantly reduced in enrichment in *spo0A::erm*, relative to the parental strain, implying positive regulation by Spo0A: CD630_07500, ModA (both $p \leq 0.05$), SsuA and OppA (both $p \leq 0.01$) (Figure 6D and Table S6). *ssuA* has an upstream Spo0A binding sequence (0A box) and is under direct positive regulation by Spo0A (Rosenbusch et al., 2012), while CD630_07500, *modA* and *oppA* are more likely to be indirectly Spo0A-regulated.

We conducted a quantitative comparison between the global proteome of these strains (Figure S7 and Table S6) and observed a highly significant ($p \leq 0.005$) reduction in expression of both SsuA (5-fold) and OppA (2-fold) in the insoluble sub-proteome of *spo0A::erm*, confirming that the reduction in enrichment of SsuA and OppA was due to a reduction in protein level. In addition, our data correlate well with known phenotypes of *spo0A::erm* and with previous proteomic and transcriptomic comparisons with 630 Δ*erm* (Fimlaid et al., 2013; Pettit et al., 2014).

Table 1. The Lipoproteome of *C. difficile* 630 Δ*erm*

Gene Name/Locus Tag	Protein Function	Predicted Lipoprotein	Myristic Acid Competition ($p \leq 0.01$)	630 Δ*erm* vs *lgt::erm* ($p \leq 0.05$)	*lgt::erm* Vs 630 Δ*erm* Shedding ($p \leq 0.05$)
appA CD630_26720	ABC-type transport system, oligopeptide-family solute-binding protein	+	+	+	+
CD630_01730	putative lipoprotein	+	+	+	
CD630_01990	putative membrane-associated nucleotidase	+	+	+	
CD630_05450	uncharacterized protein	+	+	+	+
CD630_05690	putative lipoprotein	+	+	+	
CD630_06890	putative nucleotide phosphodiesterase	+	+	+	
CD630_07470	putative lipoprotein	+	+	+	+
CD630_07500	ABC-type transport system, amino acid-family extracellular solute-binding protein	+	+	+	
CD630_08730	ABC-type transport system, sugar-family extracellular solute-binding protein	+	+	+	+
CD630_08760	ABC-type transport system, sugar-family extracellular solute-binding protein	+			+
CD630_09570	putative phage lipoprotein	+	+	+	
CD630_09990	ABC-type transport system, nitrate/sulfonate/taurine extracellular solute-binding protein	+	+	+	+
CD630_10800	putative lipoprotein	+	+	+	
CD630_11310	putative solute-binding lipoprotein	+	+	+	+
CD630_12320	putative lipoprotein	+	+	+	
CD630_15070	putative thioredoxin	+	+	+	
CD630_15090	putative lipoprotein	+	+	+	
CD630_15570	putative peptidylprolyl isomerase (PrsA2)	+	+		
CD630_15890	ABC-type transport system, sugar-family extracellular solute-binding protein	+	+	+	
CD630_16220	uncharacterized protein	+	+	+	
CD630_16530	lipoprotein	+	+	+	+
CD630_16870	uncharacterized protein	+	+	+	
CD630_17740	ABC-type transport system, amino acid-family extracellular solute-binding protein	+	+	+	
CD630_17810	putative lipoprotein	+	+	+	
CD630_18710	putative oxidoreductase Tn1549-like,CTn5-Orf30		+	+	
CD630_19300	uncharacterized protein		+		
CD630_19790	ABC-type transport system, extracellular solute-binding protein	+	+	+	+
CD630_19920	putative lipoprotein	+	+		
CD630_20290	uncharacterized protein	+	+	+	
CD630_20520	putative lipoprotein	+	+	+	

(*Continued on next page*)

Table 1. ***Continued***

Gene Name/Locus Tag	Protein Function	Predicted Lipoprotein	Myristic Acid Competition ($p \leq 0.01$)	630 Δ*erm* vs *lgt::erm* ($p \leq 0.05$)	*lgt::erm* Vs 630 Δ*erm* Shedding ($p \leq 0.05$)
CD630_21740	ABC-type transport system, cysteine/amino acid-family extracellular solute-binding protein	+	+	+	+
CD630_21770	ABC-type transport system, cysteine/amino acid-family extracellular solute-binding protein	+	+	+	+
CD630_23110	ABC-type transport system, molybdenum-like extracellular solute-binding protein	+	+		
CD630_23650	ABC-type transport system, nitrate/sulfonate/taurine extracellular solute-binding protein	+	+	+	+
CD630_24060	putative lipoprotein	+	+	+	+
CD630_25380	putative lipoprotein	+	+		
CD630_25500	ABC-type transport system, sugar-family extracellular solute-binding protein	+	+	+	+
CD630_27010	putative lipoprotein	+	+	+	+
CD630_27190	putative polysaccharide deacetylase	+	+	+	
CD630_27630	putative lipoprotein	+	+	+	
CD630_29990	ABC-type transport system, iron-family extracellular solute-binding protein	+	+	+	+
CD630_35280	ABC-type transport system, iron-family extracellular solute-binding protein	+	+	+	
CD630_36690	putative exported protein	+	+	+	+
metQ CD630_14910	ABC-type transport system, methionine-specific substrate-binding lipoprotein	+		+	+
modA CD630_08690	ABC-type transport system, molybdenum-specific extracellular solute-binding protein	+	+		
oppA CD630_08550	ABC-type transport system, oligopeptide-family extracellular solute-binding protein	+	+	+	+
potD CD630_10270	ABC-type transport system, spermidine/putrescine solute-binding protein	+	+		
prsA CD630_35000	peptidylprolyl isomerase PrsA-like (EC 5.2.1.8)	+	+	+	+
rbsB CD630_03000	ABC-type transport system, ribose-specific extracellular solute-binding protein	+	+	+	
ssuA CD630_14840	ABC-type transport system, alkane sulfonates-family extracellular solute-binding protein	+	+	+	+
ssuA2 CD630_29890	ABC-type transport system, sulfonate-family extracellular solute-binding protein	+			+

A summary of all verified lipoproteins from *C. difficile* 630 Δ*erm*, evidence for Lgt specific tagging with YnMyr is indicated (+) for the given experiments, see also Table S7.

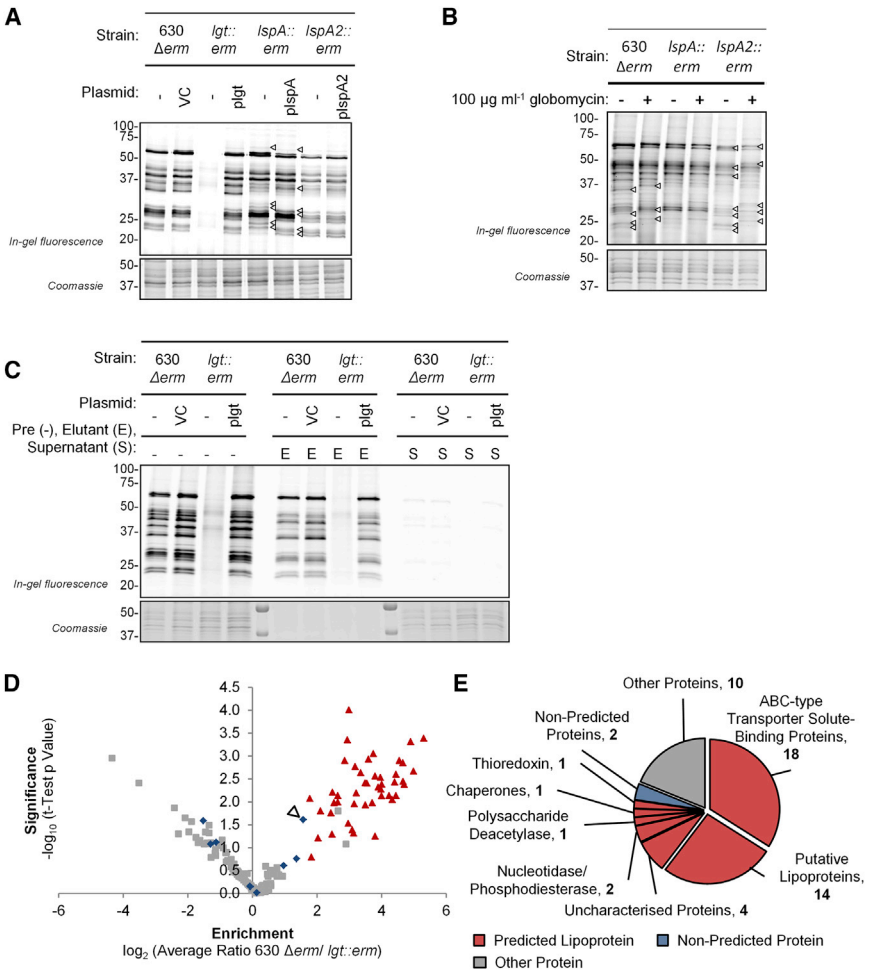

Figure 4. Investigating Lipoprotein Biogenesis in *C. difficile* 630 Δ*erm* by Metabolic Tagging

(A) The effect of inactivation of *lgt*, *lspA*, and *lspA2* on prolipoprotein processing, visualized by metabolic tagging with 25 μM YnMyr. Fluorescent bands that shift to a higher MW are indicated by arrowheads.

(B) Globomycin treatment (+) of 630 Δ*erm*, *lspA::erm*, and *lspA2::erm*. The effect of Lsp inhibition on prolipoprotein processing was assessed by metabolic tagging with 25 μM Myr. 630 Δ*erm* showed an *lspA::erm*-like phenotype on treatment, while *lspA2::erm* showed a global migration of labeled lipoproteins to a higher apparent MW, as indicated by arrowheads.

(C) Affinity enrichment of lipoproteins from 630 Δ*erm* and *lgt::erm*. Two equivalents of the elutant (E) samples were loaded relative to the input (–) and supernatant (S) samples. VC, vector control.

(D) A volcano plot showing the results of a one-sample t test ($p \leq 0.05$) comparing YnMyr-tagged proteins enriched from 630 Δ*erm* to those from *lgt::erm* (see also Figure S4), CD630_18710 is indicated. Values represent the mean of three biological replicates.

(E) The annotated functions for all proteins that displayed significantly ($p \leq 0.05$) different enrichment in (D); emphasis is placed on predicted lipoproteins. Predicted lipoproteins are colored red, competition significant (Figure 3B) proteins that are not predicted to be lipidated in blue, and other proteins in gray.

Finally, two lipoproteins, the ABC-type transporter solute-binding protein SsuA2 and CD630_19300, a highly conserved metallo-β-lactamase, showed significantly ($p \leq 0.05$) increased enrichment in *spo0A::erm* (Figure 6D). As neither gene features an upstream 0A box, they appear to be indirectly downregulated by Spo0A, suggesting repression during sporulation; however, the increase in SsuA2 may be an adaption to compensate for reduced SsuA.

DISCUSSION

Here we report the use of an alkyne-tagged analog of myristic acid (YnMyr) to profile the lipoproteome of the Gram-positive pathogen *C. difficile*. Competition between YnMyr and an excess of the natural lipid, in conjunction with quantitative proteomic analyses, generated a robust profile of the lipoproteome for 630 Δ*erm* and R20291. This is the first description of the lipoproteome of a Gram-positive bacterium, providing direct biochemical verification of lipidation for the majority of the predicted lipoproteome. YnMyr labeling was shown to occur in an Lgt-dependent manner, further validating our results. In total, we identified 74% of the predicted *C. difficile* 630 Δ*erm* lipoproteome, and an additional two novel lipoproteins (Figure 5D; Tables 1 and S7). Alignment of the lipoboxes from the *C. difficile* 630 Δ*erm* lipoproteins identified in this study revealed that the lipobox differs subtly from the consensus, with valine or threonine equally conserved in the −2 position and a more variable −3 position. In contrast, leucine is conserved in the −3 position in *B. subtilis*, while the −2 position is less conserved. In both species, glycine is favored in the −1 position (Figure S2D).

The presence of two active type II signal peptidases (LspA and LspA2) has never been reported in a Gram-positive bacterium. Utilizing genetic and chemical inactivation of the Lsps, combined with metabolic tagging with YnMyr and quantitative proteomic analysis, we have demonstrated the activity of both LspA and LspA2 in *C. difficile*. The lipoprotein biogenesis mutants expressed reduced levels of Spo0A and display a severe defect in formation of heat-resistant spores, demonstrating that complete processing of the lipoproteome is required for efficient sporulation and implicating lipoproteins in persistence and transmission of this important pathogen. A quantitative comparison between the lipoproteome of the asporogenous mutant *spo0A::erm* and the parental strain revealed significantly reduced enrichment of four ABC-transport solute-binding lipoproteins in the *spo0A::erm* mutant, indicative of regulation by Spo0A, implicating these proteins in the initiation of sporulation. We suggest that these lipoproteins may form part of a nutrient-sensing feedback mechanism, acting to confirm low nutrient availability before committing to sporulation.

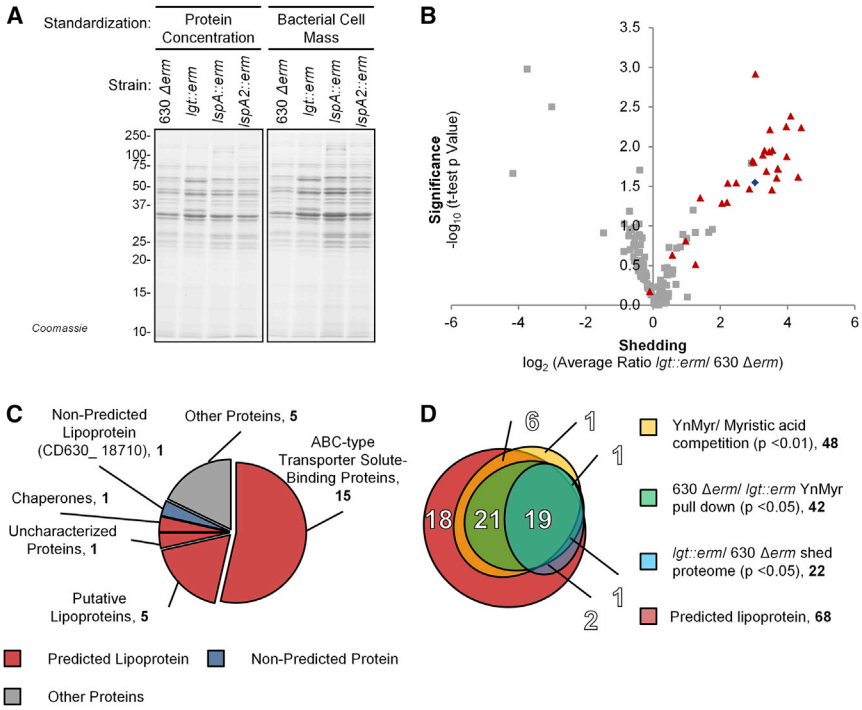

Figure 5. Lipoproteins Are Shed into the Media at an Increased Level by *lgt::erm*

(A) Proteins shed or secreted into the media by 630 Δ*erm* and the lipoprotein biogenesis mutants. Samples were standardized by protein concentration (1 mg ml^{-1}) or bacterial cell mass (30 OD_{600} ml^{-1}), see also Figure S6.

(B) A volcano plot showing the results of a one-sample t test ($p \leq 0.05$) comparing proteins shed into the media by 630 Δ*erm* to those shed by *lgt::erm*. Values represent the mean of three biological replicates.

(C) The annotated functions for all proteins that were shed at a significantly ($p \leq 0.05$) different level in (B); emphasis is placed on predicted lipoproteins. Predicted lipoproteins are colored red, competition significant (Figure 3B) proteins that are not predicted to be lipidated in blue and other proteins in gray.

(D) A Euler diagram comparing all quantitative proteomic experiments to identify *C. difficile* 630 Δ*erm* lipoproteins. 74% of the predicted lipoproteome was identified, with the majority being found in at least two independent experiments.

The reduction in Spo0A levels observed in the *lgt::erm*, *lspA::erm*, and *lspA2::erm* mutants indicates that the lipoproteins involved in this phenotype act upstream of Spo0A. We identified a number of other lipoproteins that contain other sporulation-associated domains, including a homolog of the sporulation-associated *B. subtilis* lipoprotein Med (CD630_05690). Med is required for the activation of KinD in *B. subtilis*, which initiates a phosphorelay culminating in activation of Spo0A (Banse et al., 2011). It is possible that the *C. difficile* Med homolog is required for full activity of the transmembrane kinases CD630_14920 and CD630_24920, which act directly on Spo0A (Underwood et al., 2009). As Spo0A∼P activates its own expression, a reduction in kinase activity would lead to reduced Spo0A expression, providing an explanation for this observation. Interestingly, in *B. subtilis* Lgt is required for germination, but not for sporulation (Igarashi et al., 2004), revealing further differences between the developmental pathways of these two spore-forming bacteria.

Pfam analysis of the uncharacterized lipoproteins revealed lipoproteins containing germane domains homologous to that found in the *B. subtilis* lipoprotein GerM. GerM is believed to be involved in peptidoglycan synthesis during spore development and is required for efficient spore formation and germination (Sammons et al., 1987; Slynn et al., 1994). The germane domain-containing lipoproteins in *C. difficile* may function in both sporulation and germination, and it is possible that the sporulation defect observed results from a combination of altered activity of the Med and Germane homologs. While our data do not rule out roles for lipoproteins in germination, it is highly likely that the lipoproteome plays an important role in sporulation in *C. difficile*.

In conclusion, we have demonstrated that the combination of chemical tagging of lipidation with quantitative proteomics is a powerful approach for experimental exploration and definition of the lipoproteome in a Gram-positive human pathogen.

SIGNIFICANCE

Gram-positive lipoproteins are anchored to the cell surface by an N-terminal *S*-diacylglyceryl modification. Despite the non-essential nature of the Gram-positive lipoprotein biogenesis pathway, they are frequently essential for bacterial survival and pathogenesis. The Gram-positive pathogen *C. difficile* is a leading cause of hospital-acquired infection; spores are the transmissible agent and are critical for its persistence in the environment. *C. difficile* lipoproteins have been found to play important roles in colonization and transmission; however, its lipoproteome remained poorly characterized.

Here we report the application of quantitative lipoproteomics to *C. difficile*, providing the first system-wide comparative tool to address the impact of conventional genetic and pharmacological disruption of the lipoproteome, enabling the unbiased confirmation or revision of lipoprotein assignments from bioinformatics. The usefulness of our approach is demonstrated in the first comprehensive map of the *C. difficile* lipoproteome, including that of a virulent clinical isolate. This approach provides further insights into lipoprotein biogenesis in *C. difficile*, demonstrating the activity of an accessory type II signal peptidase, LspA2. This study also provides the first evidence for the importance of lipoprotein biogenesis in sporulation, implicating lipoproteins in the transmission of this pathogen. We anticipate that the experimental framework presented here will find wide application both in *C. difficile* and in Gram-positive pathogens in general.

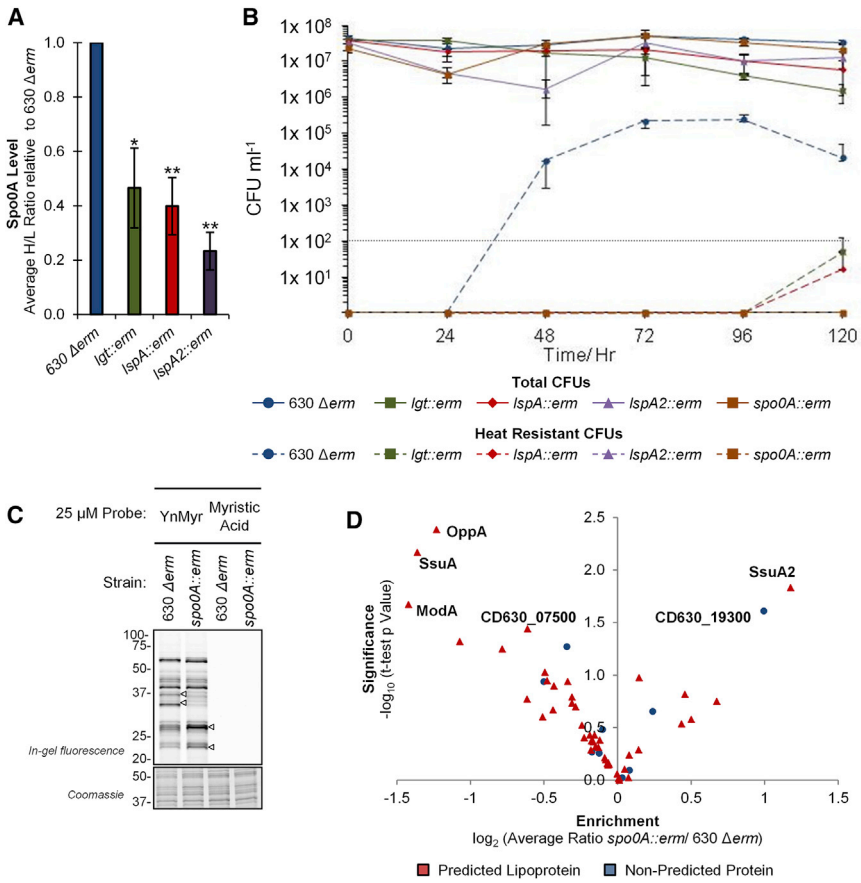

Figure 6. Lipoprotein Biogenesis Is Required for Sporulation in *C. difficile*

(A) The levels of Spo0A found in the lipoprotein biogenesis mutants is significantly reduced relative to 630 Δ*erm*, as assessed by a quantitative proteomic comparison between the global proteomes of these strains (Tables S3 and S4). Values are the average of three biological repeats, ±SD; *$p \leq 0.06$, **$p \leq 0.05$.

(B) Sporulation dynamics for the lipoprotein biogenesis pathway mutants; the asporogenous mutant *spo0A::erm* was included as a negative control. All three lipoprotein biogenesis mutants showed a significant reduction in sporulation efficiency. The zero time point was taken at the onset of the stationary phase. Values are the average for technical triplicates of biological duplicates (six values), ±SD. Values of zero were artificially set to 1 to allow plotting on a $\log_{10}$ scale, the limit of detection (100 CFU ml^{-1}) is indicated by the dotted line.

(C) Comparison between the metabolically tagged lipoproteomes (25 μM YnMyr or 25 μM myristic acid) of 630 Δ*erm* and the sporulation deficient mutant, *spo0A::erm*. Fluorescent bands that showed a noticeable change in intensity are indicated.

(D) A volcano plot showing the results of a one-sample t test ($p \leq 0.05$) comparing lipoproteins enriched from 630 Δ*erm* to those enriched from *spo0A::erm* (see also Figure S7). Values represent the mean of three biological replicates. Predicted lipoproteins are colored red and non-predicted competition significant proteins (Figure 3B) are blue.

EXPERIMENTAL PROCEDURES

The synthesis of the alkyne-tagged fatty acid probes, ClosTron mutagenesis, plasmid construction, and lists of all plasmids and primers used in this study are described in the Supplemental Information. Globomycin and the dimethyl-labeling reagents were purchased from Sigma Aldrich and used without further purification. NeutrAvidin agarose beads were purchased from Invitrogen.

Bacterial Culture

All *C. difficile* and *E. coli* strains used in this study are detailed in the Supplemental Information. *C. difficile* was routinely cultured on BHIS agar composed of 3.7% BHI (Oxoid, CM1135), 0.5% yeast extract (BD Bacto, 211713), 0.1% L-cysteine (Sigma Aldrich), 1.5% Agar (BD Bacto, 214030). Liquid cultures for metabolic labeling were performed in TY broth composed of 3% Bacto Tryptose (BD Bacto, 211713) and 2% yeast extract (BD Bacto, 210929). Liquid cultures for genetic manipulation and phenotypic assays (where indicated) were performed in BHIS broth composed of 3.7% BHI (Oxoid, CM1135), 0.5% yeast extract (BD Bacto, 210929), 0.1% L-cysteine (Sigma Aldrich). All cultures were grown at 37°C under a reducing anaerobic atmosphere (10% CO_2, 10% H_2, and 80% N_2).

Metabolic Tagging

Overnight cultures of *C. difficile* were subcultured to an optical density $(OD)_{600}$ of 0.05. For competition experiments, the subculture was immediately treated with myristic acid in DMSO to the desired concentration. Synchronously growing subcultures were allowed to grow to early exponential phase ($OD_{600} \approx 0.3$) before being treated with an alkyne-tagged fatty acid analog in DMSO; the probe and the concentration varied between experiments, with the final concentration of DMSO for each culture fixed at 1% (v/v). Typically, 10 or 25 μM YnMyr was used for metabolic labeling, and the cultures were grown to stationary phase over 6–8 hr, before cell lysis.

Proteomic Analysis

Peptide mixtures were separated on an Easy-Nano UHPLC (ultra-high-performance liquid chromatography; Thermo Scientific) equipped with an Acclaim Pepmap 100 pre-column and an EASY-Spray 50 cm × 75 μm Pepmap C_{18} column (Thermo Scientific) eluting using a gradient of 2% acetonitrile, 0.1% trifluoroacetic acid (TFA), to 98% acetonitrile, 0.1% TFA in water at a flow rate of 250 nl min^{-1}, over 2 hr. The nano-UHPLC was connected directly to a Q-Exactive Quadrupole-Orbitrap mass spectrometer (Thermo Scientific) for MS/MS analysis, via a heated EASY-Spray source (Thermo Scientific) operated at a spray voltage of 1.7 kV. The Q-Exactive was run in positive ion mode, using data-dependent (Top 10) acquisition with an isolation window of 3.0 m/z. Ions were fragmented by higher-energy collisional dissociation with normalized collision energies of 25 W; the ion target value was set to 10^6 for MS and 10^5 for MS/MS.

Data Analysis

Thermo.RAW files generated by Xcalibur were processed using MaxQuant 1.3.0.5 (Cox and Mann, 2008), searching against the corresponding database using the Andromeda search engine (Cox et al., 2011). All databases to search against were created by extracting the complete proteome of the relevant *C. difficile* strain from UniProt (630 and R20291, both 08/2013); common contaminants were included in the search. Methionine oxidation and N-terminal acetylation were set as variable modifications and cysteine *S*-carbamidomethylation as a fixed modification. For dimethyl-based quantification, the multiplicity and labels were set depending on the experiment, allowing a maximum of three labeled amino acids per peptide. A total of five modifications per peptide, two missed cleavages, and a maximum charge of +7 was allowed. A false discovery rate of 0.01 for peptides, proteins, and sites was used for identification; the minimum peptide length allowed was seven amino acids. For protein identification, the minimum number of peptides and razor + unique peptides allowed was set to 1; both razor and unique peptides were used for

quantification. Only proteins that were quantified in all biological replicates were used for further analysis. Data were filtered to remove common contaminants, normalized to the median, and statistical testing was performed using Perseus 1.4.0.8. Protein annotations were imported from the UniProt and Pfam databases, and the data were exported to Microsoft Excel 2010 for further analysis. The mass spectrometry proteomics data have been deposited in the ProteomeXchange Consortium (Vizcaino et al., 2014) via the PRIDE partner repository with the dataset identifier PRIDE: PXD002426.

ACCESSION NUMBERS

The accession number for the proteomics data reported in this paper is PRIDE: PXD002426.

SUPPLEMENTAL INFORMATION

Supplemental Information includes Supplemental Experimental Procedures, seven figures, and seven tables and can be found with this article online at http://dx.doi.org/10.1016/j.chembiol.2015.10.006.

AUTHOR CONTRIBUTIONS

T.C. conducted the chemical synthesis, metabolic tagging, and proteomics experiments; A.K.-S. and S.M. constructed the *lgt*, *lspA*, and *lspA2* mutants; E.T. and N.F. conceived the study; T.C., N.F., and E.T. wrote the manuscript, which was approved by all authors.

ACKNOWLEDGMENTS

T.C. was funded by an EPSRC grant to the Institute of Chemical Biology, Imperial College London. A.K.-S. was funded by a European Union Seventh Framework Program (EU MCN Grant agreement 237942). We thank Remigiusz Serwa for his valuable support and critical reading of the manuscript.

Received: July 16, 2015
Revised: September 28, 2015
Accepted: October 1, 2015
Published: November 12, 2015

REFERENCES

Alloing, G., de Philip, P., and Claverys, J.P. (1994). Three highly homologous membrane-bound lipoproteins participate in oligopeptide transport by the Ami system of the gram-positive *Streptococcus pneumoniae*. J. Mol. Biol. *241*, 44–58.

Banse, A.V., Hobbs, E.C., and Losick, R. (2011). Phosphorylation of Spo0A by the histidine kinase KinD requires the lipoprotein med in *Bacillus subtilis*. J. Bacteriol. *193*, 3949–3955.

Baumgartner, M., Karst, U., Gerstel, B., Loessner, M., Wehland, J., and Jansch, L. (2007). Inactivation of Lgt allows systematic characterization of lipoproteins from *Listeria monocytogenes*. J. Bacteriol. *189*, 313–324.

Berry, A.F., Heal, W.P., Tarafder, A.K., Tolmachova, T., Baron, R.A., Seabra, M.C., and Tate, E.W. (2010). Rapid multilabel detection of geranylgeranylated proteins by using bioorthogonal ligation chemistry. Chembiochem *11*, 771–773.

Blanc, L., Castanier, R., Mishra, A.K., Ray, A., Besra, G.S., Sutcliffe, I., Vercellone, A., and Nigou, J. (2013). Gram-positive bacterial lipoglycans based on a glycosylated diacylglycerol lipid anchor are microbe-associated molecular patterns recognized by TLR2. PLoS One *8*, e81593.

Boersema, P.J., Raijmakers, R., Lemeer, S., Mohammed, S., and Heck, A.J. (2009). Multiplex peptide stable isotope dimethyl labeling for quantitative proteomics. Nat. Protoc. *4*, 484–494.

Broncel, M., Serwa, R.A., Ciepla, P., Krause, E., Dallman, M.J., Magee, A.I., and Tate, E.W. (2015). Multifunctional reagents for quantitative proteome-wide analysis of protein modification in human cells and dynamic profiling of protein lipidation during vertebrate development. Angew. Chem. Int. Ed. Engl. *54*, 5948–5951.

Buddelmeijer, N. (2015). The molecular mechanism of bacterial lipoprotein modification–how, when and why? FEMS Microbiol. Rev. *39*, 246–261.

Charron, G., Zhang, M.M., Yount, J.S., Wilson, J., Raghavan, A.S., Shamir, E., and Hang, H.C. (2009). Robust fluorescent detection of protein fatty-acylation with chemical reporters. J. Am. Chem. Soc. *131*, 4967–4975.

Charron, G., Li, M.M., MacDonald, M.R., and Hang, H.C. (2013). Prenylome profiling reveals S-farnesylation is crucial for membrane targeting and antiviral activity of ZAP long-isoform. Proc. Natl. Acad. Sci. USA *110*, 11085–11090.

Chimalapati, S., Cohen, J.M., Camberlein, E., MacDonald, N., Durmort, C., Vernet, T., Hermans, P.W., Mitchell, T., and Brown, J.S. (2012). Effects of deletion of the *Streptococcus pneumoniae* lipoprotein diacylglyceryl transferase gene lgt on ABC transporter function and on growth in vivo. PLoS One *7*, e41393.

Ciepla, P., Konitsiotis, A.D., Serwa, R.A., Masumoto, N., Leong, W.P., Dallman, M.J., Magee, A.I., and Tate, E.W. (2014). New chemical probes targeting cholesterylation of Sonic Hedgehog in human cells and zebrafish. Chem. Sci. *5*, 4249–4259.

Cox, J., and Mann, M. (2008). MaxQuant enables high peptide identification rates, individualized p.p.b.-range mass accuracies and proteome-wide protein quantification. Nat. Biotechnol. *26*, 1367–1372.

Cox, J., Neuhauser, N., Michalski, A., Scheltema, R.A., Olsen, J.V., and Mann, M. (2011). Andromeda: a peptide search engine integrated into the MaxQuant environment. J. Proteome Res. *10*, 1794–1805.

Cox, A.D., St Michael, F., Aubry, A., Cairns, C.M., Strong, P.C., Hayes, A.C., and Logan, S.M. (2013). Investigating the candidacy of a lipoteichoic acid-based glycoconjugate as a vaccine to combat *Clostridium difficile* infection. Glycoconj. J. *30*, 843–855.

Deakin, L.J., Clare, S., Fagan, R.P., Dawson, L.F., Pickard, D.J., West, M.R., Wren, B.W., Fairweather, N.F., Dougan, G., and Lawley, T.D. (2012). The *Clostridium difficile* spo0A gene is a persistence and transmission factor. Infect. Immun. *80*, 2704–2711.

Edwards, A.N., and McBride, S.M. (2014). Initiation of sporulation in *Clostridium difficile*: a twist on the classic model. FEMS Microbiol. Lett. *358*, 110–118.

Edwards, A.N., Nawrocki, K.L., and McBride, S.M. (2014). Conserved oligopeptide permeases modulate sporulation initiation in *Clostridium difficile*. Infect. Immun. *82*, 4276–4291.

Evans, C.T., and Safdar, N. (2015). Current trends in the epidemiology and outcomes of *Clostridium difficile* infection. Clin. Infect. Dis. *60* (*Suppl 2*), S66–S71.

Fagan, R.P., and Fairweather, N.F. (2011). *Clostridium difficile* has two parallel and essential Sec secretion systems. J. Biol. Chem. *286*, 27483–27493.

Fimlaid, K.A., Bond, J.P., Schutz, K.C., Putnam, E.E., Leung, J.M., Lawley, T.D., and Shen, A. (2013). Global analysis of the sporulation pathway of *Clostridium difficile*. PLoS Genet. *9*, e1003660.

Gerding, D.N., Muto, C.A., and Owens, R.C. (2008). Measures to control and prevent *Clostridium difficile* infection. Clin. Infect. Dis. *46* (*Suppl 1*), S43–S49.

Hayashi, S., Chang, S.Y., Chang, S., Giam, C.Z., and Wu, H.C. (1985). Modification and processing of internalized signal sequences of prolipoprotein in *Escherichia coli* and in *Bacillus subtilis*. J. Biol. Chem. *260*, 5753–5759.

Heap, J.T., Pennington, O.J., Cartman, S.T., Carter, G.P., and Minton, N.P. (2007). The ClosTron: a universal gene knock-out system for the genus *Clostridium*. J. Microbiol. Methods *70*, 452–464.

Hussain, M., Ichihara, S., and Mizushima, S. (1980). Accumulation of glyceride-containing precursor of the outer membrane lipoprotein in the cytoplasmic membrane of *Escherichia coli* treated with globomycin. J. Biol. Chem. *255*, 3707–3712.

Hutchings, M.I., Palmer, T., Harrington, D.J., and Sutcliffe, I.C. (2009). Lipoprotein biogenesis in gram-positive bacteria: knowing when to hold 'em, knowing when to fold 'em. Trends Microbiol. *17*, 13–21.

Igarashi, T., Setlow, B., Paidhungat, M., and Setlow, P. (2004). Effects of a gerF (lgt) mutation on the germination of spores of *Bacillus subtilis*. J. Bacteriol. *186*, 2984–2991.

Jank, T., and Aktories, K. (2008). Structure and mode of action of clostridial glucosylating toxins: the ABCD model. Trends Microbiol. *16*, 222–229.

Kontinen, V.P., and Sarvas, M. (1993). The PrsA lipoprotein is essential for protein secretion in *Bacillus subtilis* and sets a limit for high-level secretion. Mol. Microbiol. *8*, 727–737.

Kovacs-Simon, A., Titball, R.W., and Michell, S.L. (2011). Lipoproteins of bacterial pathogens. Infect. Immun. *79*, 548–561.

Kovacs-Simon, A., Leuzzi, R., Kasendra, M., Minton, N., Titball, R.W., and Michell, S.L. (2014). Lipoprotein CD0873 is a novel adhesin of *Clostridium difficile*. J. Infect. Dis. *210*, 274–284.

Kuipers, E.J., and Surawicz, C.M. (2008). *Clostridium difficile* infection. Lancet *371*, 1486–1488.

Lawley, T.D., Clare, S., Walker, A.W., Goulding, D., Stabler, R.A., Croucher, N., Mastroeni, P., Scott, P., Raisen, C., Mottram, L., et al. (2009). Antibiotic treatment of clostridium difficile carrier mice triggers a supershedder state, spore-mediated transmission, and severe disease in immunocompromised hosts. Infect. Immun. *77*, 3661–3669.

Li, N., Kuo, C.L., Paniagua, G., van den Elst, H., Verdoes, M., Willems, L.I., van der Linden, W.A., Ruben, M., van Genderen, E., Gubbens, J., et al. (2013). Relative quantification of proteasome activity by activity-based protein profiling and LC-MS/MS. Nat. Protoc. *8*, 1155–1168.

Martin, B.R., Wang, C., Adibekian, A., Tully, S.E., and Cravatt, B.F. (2012). Global profiling of dynamic protein palmitoylation. Nat. Methods *9*, 84–89.

Nakayama, H., Kurokawa, K., and Lee, B.L. (2012). Lipoproteins in bacteria: structures and biosynthetic pathways. FEBS J. *279*, 4247–4268.

Nielsen, J.B., and Lampen, J.O. (1982). Membrane-bound penicillinases in gram-positive bacteria. J. Biol. Chem. *257*, 4490–4495.

Okugawa, S., Moayeri, M., Pomerantsev, A.P., Sastalla, I., Crown, D., Gupta, P.K., and Leppla, S.H. (2012). Lipoprotein biosynthesis by prolipoprotein diacylglyceryl transferase is required for efficient spore germination and full virulence of *Bacillus anthracis*. Mol. Microbiol. *83*, 96–109.

Pettit, L.J., Browne, H.P., Yu, L., Smits, W.K., Fagan, R.P., Barquist, L., Martin, M.J., Goulding, D., Duncan, S.H., Flint, H.J., et al. (2014). Functional genomics reveals that *Clostridium difficile* Spo0A coordinates sporulation, virulence and metabolism. BMC Genomics *15*, 160.

Pribyl, T., Moche, M., Dreisbach, A., Bijlsma, J.J., Saleh, M., Abdullah, M.R., Hecker, M., van Dijl, J.M., Becher, D., and Hammerschmidt, S. (2014). Influence of impaired lipoprotein biogenesis on surface and exoproteome of *Streptococcus pneumoniae*. J. Proteome Res. *13*, 650–667.

Rahman, O., Cummings, S.P., Harrington, D.J., and Sutcliffe, I.C. (2008). Methods for the bioinformatic identification of bacterial lipoproteins encoded in the genomes of gram-positive bacteria. World J. Microbiol. Biotechnol *24*, 2377–2382.

Rangan, K.J., Yang, Y.Y., Charron, G., and Hang, H.C. (2010). Rapid visualization and large-scale profiling of bacterial lipoproteins with chemical reporters. J. Am. Chem. Soc. *132*, 10628–10629.

Reglier-Poupet, H., Frehel, C., Dubail, I., Beretti, J.L., Berche, P., Charbit, A., and Raynaud, C. (2003). Maturation of lipoproteins by type II signal peptidase is required for phagosomal escape of *Listeria monocytogenes*. J. Biol. Chem. *278*, 49469–49477.

Reid, C.W., Vinogradov, E., Li, J., Jarrell, H.C., Logan, S.M., and Brisson, J.R. (2012). Structural characterization of surface glycans from *Clostridium difficile*. Carbohydr. Res. *354*, 65–73.

Rosenbusch, K.E., Bakker, D., Kuijper, E.J., and Smits, W.K. (2012). C. difficile 630Δerm Spo0A regulates sporulation, but does not contribute to toxin production, by direct high-affinity binding to target DNA. PLoS One *7*, e48608.

Sammons, R.L., Slynn, G.M., and Smith, D.A. (1987). Genetical and molecular studies on gerM, a new developmental locus of *Bacillus subtilis*. J. Gen. Microbiol. *133*, 3299–3312.

Sankaran, K., and Wu, H.C. (1994). Lipid modification of bacterial prolipoprotein. Transfer of diacylglyceryl moiety from phosphatidylglycerol. J. Biol. Chem. *269*, 19701–19706.

Slynn, G.M., Sammons, R.L., Smith, D.A., Moir, A., and Corfe, B.M. (1994). Molecular genetical and phenotypical analysis of the gerM spore germination gene of *Bacillus subtilis* 168. FEMS Microbiol. Lett. *121*, 315–320.

Stabler, R.A., He, M., Dawson, L., Martin, M., Valiente, E., Corton, C., Lawley, T.D., Sebaihia, M., Quail, M.A., Rose, G., et al. (2009). Comparative genome and phenotypic analysis of *Clostridium difficile* 027 strains provides insight into the evolution of a hypervirulent bacterium. Genome Biol. *10*, R102.

Tate, E.W., Kalesh, K.A., Lanyon-Hogg, T., Storck, E.M., and Thinon, E. (2015). Global profiling of protein lipidation using chemical proteomic technologies. Curr. Opin. Chem. Biol. *24*, 48–57.

Thinon, E., Serwa, R.A., Broncel, M., Brannigan, J.A., Brassat, U., Wright, M.H., Heal, W.P., Wilkinson, A.J., Mann, D.J., and Tate, E.W. (2014). Global profiling of co- and post-translationally N-myristoylated proteomes in human cells. Nat. Commun. *5*, 4919.

Underwood, S., Guan, S., Vijayasubhash, V., Baines, S.D., Graham, L., Lewis, R.J., Wilcox, M.H., and Stephenson, K. (2009). Characterization of the sporulation initiation pathway of *Clostridium difficile* and its role in toxin production. J. Bacteriol. *191*, 7296–7305.

Vizcaino, J.A., Deutsch, E.W., Wang, R., Csordas, A., Reisinger, F., Rios, D., Dianes, J.A., Sun, Z., Farrah, T., Bandeira, N., et al. (2014). ProteomeXchange provides globally coordinated proteomics data submission and dissemination. Nat. Biotechnol. *32*, 223–226.

Widdick, D.A., Hicks, M.G., Thompson, B.J., Tschumi, A., Chandra, G., Sutcliffe, I.C., Brulle, J.K., Sander, P., Palmer, T., and Hutchings, M.I. (2011). Dissecting the complete lipoprotein biogenesis pathway in *Streptomyces scabies*. Mol. Microbiol. *80*, 1395–1412.

Wright, M.H., Clough, B., Rackham, M.D., Rangachari, K., Brannigan, J.A., Grainger, M., Moss, D.K., Bottrill, A.R., Heal, W.P., Broncel, M., et al. (2014). Validation of N-myristoyltransferase as an antimalarial drug target using an integrated chemical biology approach. Nat. Chem. *6*, 112–121.

Yang, Y.Y., Ascano, J.M., and Hang, H.C. (2010). Bioorthogonal chemical reporters for monitoring protein acetylation. J. Am. Chem. Soc. *132*, 3640–3641.